The Proline-Rich N-Terminal Sequence of Calcineurin Aβ Determines Substrate Binding

Susann Kilka, Frank Erdmann, Alexander Migdoll, Gunter Fischer,* and Matthias Weiwad*

Max Planck Research Unit for Enzymology of Protein Folding, Weinbergweg 22, D-06120 Halle/Saale, Germany

Received October 15, 2008; Revised Manuscript Received January 20, 2009

ABSTRACT: Three different genes of catalytic subunit A of the Ca^{2+}-dependent serine/threonine protein phosphatase calcineurin (CaN) are encoded in the human genome forming heterodimers with regulatory subunit B. Even though physiological roles of CaN have been investigated extensively, less is known about the specific functions of the different catalytic isoforms. In this study, all human CaN holoenzymes containing either the α, β, or γ isoform of the catalytic subunit (CaN α, β, or γ, respectively) were expressed for the first time. Comparative kinetic analysis of the dephosphorylation of five specific CaN substrates provided evidence that the distinct isoforms of the catalytic subunit confer substrate specificities to the holoenzymes. CaN α dephosphorylates the transcription factor Elk-1 with 7- and 2-fold higher catalytic efficiencies than the β and γ isoforms, respectively. CaN γ exhibits the highest k_{cat}/K_m value for DARPP-32, whereas the catalytic efficiencies for the dephosphorylation of NFAT and RII peptide were 3- and 5-fold lower, respectively, when compared with the other isoforms. Elk-1 and NFAT reporter gene activity measurements revealed even more pronounced substrate preferences of CaNA isoforms. Moreover, kinetic analysis demonstrated that CaN β exhibits for all tested protein substrates the lowest K_m values. Enzymatic characterization of the CaN $\beta^{P14G/P18G}$ variant as well as the N-terminal truncated form CaN β^{22-524} revealed that the proline-rich sequence of CaN β is involved in substrate recognition. CaN β^{22-524} exhibits an at least 4-fold decreased substrate affinity and a 5-fold increased turnover number. Since this study demonstrates that all CaN isoforms display the same cytoplasmic subcellular distribution and are expressed in each tested cell line, differences in substrate specificities may determine specific physiological functions of the distinct isoforms.

The protein phosphatase calcineurin (CaN,[1] PP2B) possesses a unique position among serine/threonine protein phosphatases in that its activity is controlled by the second messenger calcium and the calcium binding protein calmodulin (CaM). Besides its tight regulation by calcium, CaN exhibits relatively narrow substrate specificity when compared with related protein phosphatases. These special regulatory and biochemical properties confer CaN a central role in many physiological processes, including immune response, apoptosis, muscle differentiation, bone formation, and neuronal signaling (*1*−*3*).

The highest expression level of CaN was observed in brain tissue, where it is involved in diverse neuronal processes, such as long-term memory (*4*), axon formation (*5*), and neurotransmitter release (*6*). In brain, CaN dephosphorylates the dopamine- and cAMP-regulated phosphoprotein (DARPP-32), an endogenous inhibitor of protein phosphatase 1 (PP1), at threonine 34, which subsequently results in activation of PP1 (*7*). In contrast, inhibition of neuronal CaN activity was correlated with an increase in the level of hyperphosphorylation of the microtubule-associated protein Tau, which leads to loss of microtubule binding and aggregation of Tau in the brain and finally to typical symptoms of Alzheimer's disease (*8, 9*).

Transcription factors of the nuclear factor of activated T cells (NFAT) family represent major substrates of CaN in cells of the immune system, cardiomyocytes, and skeletal muscle. Dephosphorylation of NFAT leads to conformational changes resulting in exposure of a nuclear translocation signal and an increased affinity for specific DNA sequences and therefore in the induction of the transcription of interleukin 2, 3, and 4; interferon γ; and tumor necrosis factor α (*10*−*15*). Calcineurin activity and thus NFAT dephosphorylation are inhibited by the clinically relevant immunosuppressive drugs, cyclosporine A (CsA) and FK506 (*16*). However, the drugs alone do not inhibit the enzymatic activity of CaN. Inhibition by CsA and FK506 occurs only after formation of a complex with their respective target proteins, the cyclophilins, and the FK506-binding proteins through a gain-of-function mechanism. Beside NFAT, CaN dephosphorylates and thus directly regulates further transcription factors, like Ets-like gene 1 (Elk-1) and myocyte enhancer factor 2 (*17*).

CaN is a heterodimeric enzyme composed of an ~60 kDa catalytic subunit, CaNA, and a 19 kDa regulatory subunit,

* To whom correspondence should be addressed: Weinbergweg 22, D-06120 Halle/Saale, Germany. Phone: (0345) 55-22800. Fax: (0345) 55-11972. E-mail: fischer@enzyme-halle.mpg.de or weiwad@enzyme-halle.mpg.de.

[1] Abbreviations: CaN, calcineurin; CaNA, catalytic subunit of CaN; CaNB, regulatory subunit of CaN; CaN α, β, and γ, CaN heterodimeric enzymes containing the different isoforms of the catalytic subunit; CaM, calmodulin; DARPP-32, dopamine- and cAMP-regulated phosphoprotein; NFAT, nuclear factor of activated T cells; Elk-1, Ets-like gene 1; CREB, cAMP response element binding protein; CsA, cyclosporine A; pNPP, 4-nitrophenyl phosphate.

10.1021/bi8019355 CCC: $40.75
Published on Web 01/20/2009

CaNB (*18*). The catalytic subunit consists of a catalytic domain, a CaNB binding domain, a CaM interaction motif, and a C-terminal autoinhibitory region (*19*). The regulatory subunit is a CaM-like EF-hand protein (*20*). In the human genome, CaNA exists in three distinct isoforms (α, β, and γ) that are encoded by distinct genes on different chromosomes. The isoforms may contribute to a more precise regulation of diverse CaN functions in different tissues. However, there are only a few examples of specific functions of the three isoforms. In rodents, CaNA γ was identified as being the predominantly expressed isoform in testis, whereas in humans, the isoform was also found in brain where it is directly linked to schizophrenia pathogenesis and bipolar disorder (*21*−*23*). Even though CaNA α and β are ubiquitously expressed, distinct physiological functions were proposed. CaNA β plays a critical role in T cell development, whereas CaNA α is responsible for the antigen-specific T cell response (*24, 25*). Moreover, upregulation of the α isoform was shown in the diabetic kidney. In brain, the loss of the α isoform abolishes synaptic depotentiation (*26*). CaNA α knockout mice are smaller and infertile and live only a few weeks (*27*). In contrast, β-null mice exhibited an impaired cardiac hypertrophic response but are able to live and are fertile (*28*). Hence, although the three CaNA isoforms are largely homologous and only the N- and C-terminal sequences are different, the isoforms have distinct tissue-specific roles, and most tissues cannot compensate for the loss of one isoform (*29*). However, no isoform-specific substrates or cell-type-specific differences in the regulation of the activity of the CaNA isoforms were identified so far. In contrast to the α and γ isoforms, the N-terminus of the β isoform contains a polyproline motif that may represent a protein−protein interaction motif (*30*). Thus, it was proposed that this region may contribute to differential substrate specificities of the isoforms (*31*). However, substrates that are exclusively dephosphorylated by the β isoform remain to be uncovered.

To reveal different functions of CaN isoforms, we expressed for the first time all three human isoforms and performed a comparative analysis by determining kinetic constants for the dephosphorylation of the specific CaN substrates NFAT, DARPP-32, Elk-1, Tau, and RII peptide. Thereby, the influence of the N-terminal proline-rich sequence of CaNA β on catalytic properties was investigated.

MATERIALS AND METHODS

Materials. Streptavidin-coated scintillation plates were from Wallac (Turku, Finland). The biotinylated 19-residue peptide (RII peptide) of the RII subunit of bovine cAMP-dependent protein kinase A (DLDVPIPGRFDRRVSVAAE-OH) was from Bachem (Weil am Rhein, Germany). [γ-^{33}P]ATP was purchased from Hartmann Analytics (Braunschweig, Germany). Rabbit anti-CaNA α IgG and rabbit anti-actin were ordered from Sigma (St. Louis, MO). Rabbit anti-CaNA β was from Millipore (Billerica, MA). Goat anti-CaNA γ (C17) was purchased from Santa Cruz (Santa Cruz, CA). Peroxidase-conjugated mouse anti-rabbit IgG and donkey anti-goat IgG were from Dianova (Hamburg, Germany).

Proteins. cAMP-dependent protein kinase A (PKA), extracellular signal-regulated kinase 2 (ERK-2), and glycogen synthase kinase 3β (GSK-3β) were obtained from NEB (Beverly, MA). Rat recombinant DARPP-32 was purchased from Calbiochem (La Jolla, CA). Human GST-fused Elk-1 was from Cell Signaling (Beverly, MA). NFATc1$^{2-298}$ was obtained from Cell Sciences (Canton, MA). The tandem expression construct of His$_6$-CaNA α and CaNB 1 in pET15a and the yeast N-myristoyltransferase in pBB131 were published (*32*). CaNA β, CaNA β$^{22-524}$, and CaNA γ were cloned instead of CaNA α in the vector via restriction enzymes *Nde*I and *Xho*I using the following primers: CaNA β forward primer, 5′-GATCGACATATGGCCGCCCCGGAGCCGGCC-3′; CaNA β reverse primer, 5′-AGCTAGCTCGAGGATTGACTGGGCAGTATGGTTGCC-3′; CaNA β$^{22-524}$ forward primer, 5′-GATCGACATATGGGGGCTGACCGCGTCGTC-3′; CaNA β$^{22-524}$ reverse primer, 5′-GATCGACTCGAGTCACTGGGCAGTATGGTT-3′; CaNA γ forward primer, 5′-GATCGACATATGTCCGGGAGGCGCTTCCACCTC-3′; and CaNA γ reverse primer, 5′-AGCTAGCTCGAGGATTGATGAATGGGCTTTCTTCCC-3′. To obtain the CaNA β$^{P14G/P18G}$ variant, a site-directed mutagenesis of CaNA β was performed using the QuikChange site-directed mutagenesis kit from Stratagene: CaNA β$^{P14G/P18G}$ forward primer, 5′-GCACCGCCCCCAGGCCCGCCCCCGGGGCCCCCTCCCGGG-3′; and CaNA β$^{P14G/P18G}$ reverse primer, 5′-CCCGGGAGGGGGCCCCGGGGGCGGGCCTGGGGGCGGTGC-3′. CaNA γ was cloned in the pET15b vector with either CaNB 1 or CaNB 2. Therefore, the B 1 subunit was replaced by CaNB 2: CaNB 2 forward primer, 5′-GATCGACTCGAGGAGATATACATATGGGAAACGAGGCC-3′; and CaNB 2 reverse primer, 5′-AGCTAGGGATCCTGATACGATGAGGACCAGC-3′. Purification of the CaN isoforms coexpressed with the *N*-myristoyltransferase was performed according to the method of Mondragon et al. (*32*).

Overexpression of CaNA α, CaNA β, CaNA γ, and CaNA β$^{22-524}$ in human cell lines was performed using the pmaxFP-Red-C vector (Amaxa, Cologne, Germany). The isoforms were cloned via restriction enzymes *Xho*I and *Bam*HI using the following primers: CaNA α forward primer, 5′-GATCGACTCGAGCAATGTCCGAGCCCAAGGCA-3′; CaNA α reverse primer, 5′-GATCGAGGATCCTCACTGAATATTGCTGCT-3′; CaNA β forward primer, 5′-GATCGACTCGAGCAATGGCCGCCCCGGAGCCG-3′; CaNA β reverse primer, 5′-GATCGAGGATCCTCACTGGGCAGTATGGTT-3′; CaNA γ forward primer, 5′-GATCGACTCGAGCAATGTCCGGGAGGCGCTTC-3′; CaNA γ reverse primer, 5′-GATCGAGGATCCTCATGAATGGGCTTTCTT-3′; CaNA β$^{22-524}$ forward primer, 5′-GATCGACTCGAGCAGGGGCTGACCGCGTCGTC-3′; and CaNA β$^{22-524}$ reverse primer, 5′-GATCGAGGATCCTCACTGGGCAGTATGGTT-3′.

Far-UV CD Spectroscopy. The CD measurements were performed on a Jasco J-710 CD spectrometer (Gross-Umstadt, Germany) in a 0.1 cm quartz cuvette with 20 mM Tris-HCl buffer (pH 7.5) at wavelengths of 190−300 nm. The temperature varied from 4 to 95 °C. The corresponding buffer spectra were subtracted.

Calcineurin Activity Assays. (A) CaN Activity toward 4-Nitrophenyl Phosphate (pNPP). CaN activity was measured in 50 mM Tris-HCl (pH 8.0), 30 mM $MgCl_2$, 5 mM $CaCl_2$, 0.1 mg/mL BSA, 0.5 mM DTT, 1 μM CaM, and 10 mM pNPP at 25 °C. To determine the kinetic constants, 40 nM CaN α, CaN β, CaNA β$^{22-524}$, and CaN γ were measured

in the presence of increasing pNPP concentrations from 0 to 120 mM. Free *p*-nitrophenolate was measured at 405 nm. Initial slopes of the reactions were determined by linear regression.

(B) Phosphorylation of CaN Substrates. The biotinylated and nonbiotinylated RII peptide of 19-mer regulatory subunit RII (biot-DLDVPIRGRFDRRVSVAAE-OH) of PKA were phosphorylated at the serine residue using the catalytic subunit of PKA. The reaction mixture for the phosphorylation of the biotinylated RII peptide contained 600 μM RII peptide, 100 μCi (*32*) of ATP, 650 μM ATP, and 17.5 kilounits of PKA in a final volume of 30 μL of PKA buffer (NEB). The mixture was incubated at 30 °C for 16 h. The nonbiotinylated RII peptide was phosphorylated using 1 mM RII peptide, 1 mM ATP, and 50 kilounits of PKA in a final volume of 100 μL of PKA buffer. The mixture was incubated at 30 °C for 6 h. Stoichiometric phosphorylation was verified by mass spectrometry. Both peptides were separated from ATP by a 1 mL RP-C2 cleanup extraction column (Amchro).

The phosphorylation of NFAT was performed in a reaction volume of 60 μL in the presence of 30 μM NFAT, 0.7 μM [γ-^{33}P]ATP, 190 μM ATP, 2500 units of GSK-3β, 12500 units of PKA, 10 mM $MgCl_2$, 6 μL of PKA buffer (NEB), and 2 mM DTT overnight at 30 °C. To phosphorylate the DARPP-32, 30 μM DARPP-32 was incubated in 60 μL with 0.8 μM [γ-^{33}P]ATP, 200 μM ATP, 17500 units of PKA, 10 mM $MgCl_2$, 6 μL of PKA buffer (NEB), and 2 mM DTT at 30 °C overnight. Elk-1 was phosphorylated in a 50 μL reaction mixture containing 55 μM Elk-1, 1 μM [γ-^{33}P]ATP, 195 μM ATP, 240 units of Erk-2, 10 mM $MgCl_2$, 2.4 μL of MAPK buffer, and 2 mM DTT at 30 °C overnight. Tau was phosphorylated in 60 μL using 11 μM Tau, 1 μM [γ-^{33}P]ATP, 190 μM ATP, 2500 units of GSK-3β, 240 units of Erk-2, 10 mM $MgCl_2$, 6 μL of PKA buffer (NEB), and 2 mM DTT at 30 °C overnight. To separate the phosphorylated protein from free ATP, samples were purified using Mini Quick Spin Columns (Roche, Mannheim, Germany).

(C) Dephosphorylation of ^{33}P-Labeled RII Peptide. Calcineurin activity was measured using the scintillation proximity assay according to the method of Baumgrass (*33*). CaM (150 nM) and CaN (15 nM) were preincubated in buffer [40 mM Tris-HCl (pH 7.5), 100 mM NaCl, 6 mM $MgCl_2$, 1 mM $CaCl_2$, 500 μM DTT, and 100 μg/mL bovine serum albumin] for 10 min at room temperature in a 96-well microtiter plate (Costar). Subsequently, 100 pmol of ^{33}P-labeled RII peptide was added to each well in a total assay volume of 100 μL and incubated for 30 min at 30 °C. Then, 90 μL of the reaction mixture was transferred into a streptavidin-coated scintillation well (Perkin-Elmer, Boston, MA), and the biotinylated RII peptide was allowed to bind onto streptavidin for 20 min at room temperature. The wells were washed twice, and RII peptide associated ^{33}P was measured in a MicroBeta top counter (Wallac). Values of K_m and V_{max} were calculated by fitting of the hyperbolic curves to the Michaelis−Menten equation.

To determine the kinetic constants of CaN isoforms, biotinylated ^{33}P-labeled RII peptide was used at constant concentrations of 0.1 μM, whereas phosphorylated nonbiotinylated RII peptide was added in the concentration range of 0.5−30 μM. The assay mixture containing 15 nM CaN α, β, β^{22-524}, or γ and 150 nM CaM was incubated for 1 h at 30 °C in PKA buffer. Bound ^{33}P-labeled RII peptide was measured after incubation for 20 min in a streptavidin-coated scintillation plate.

(D) Dephosphorylation of Protein Substrates. CaN activity was measured by the release of ^{33}P from ^{33}P-labeled substrates. The enzyme was assayed in a reaction mixture (10 μL) containing 40 mM Tris-HCl (pH 7.5), 6 mM $MgCl_2$, 100 mM NaCl, 1 mM $CaCl_2$, 500 μM DTT, 100 μg/mL BSA, 100 nM CaM, an appropriate amount of CaN (5−70 nM), and various concentrations of ^{33}P-labeled substrates. The concentrations of phosphorylated protein substrates were calculated from the radioactivity.

The dephosphorylation reaction was started by the addition of ^{33}P-labeled substrate. After incubation for times ranging from 1 to 90 min, proteins were precipitated by addition of 10 mg/mL BSA and 20 μL of 20% TCA. After incubation for 15 min on ice, samples were centrifuged for 15 min at 15000*g* and measured by liquid scintillation counting. Values of K_m and V_{max} were calculated by fitting of the hyperbolic curves to the Michaelis−Menten equation.

Cell Culture. Neuroblastoma cell line SH-SY5Y was cultured in DMEM (Biochrom, Berlin, Germany) supplemented with 2 mM L-glutamine and 10% (v/v) heat-inactivated FCS in a humidified incubator at 37 °C in 10% (v/v) CO_2. For experiments, SH-SY5Y cells were seeded at a density of 5×10^6 cells/mL in six-well plates.

Production of the Cell Lysates. The different human cell lines were cultured in 150 cm^2 cell culture flasks to a confluency of 80% and harvested. After being washed with PBS, cells were taken up in 10 mM Tris-HCl (pH 7.5) with protease inhibitors and sonicated. Protein concentrations were determined by a Bradford assay and diluted to 1 mg/mL.

Transfection of the SH-SY5Y Cell Line. The transfection of neuroblastoma cell line SH-SY5Y with the CaN/pmaxFP-Red-C constructs was performed using Lipofectamine 2000 (Invitrogen) in six-well plates following the manufacturer's instruction of plasmid transfection.

NFAT Reporter Gene Activity. To determine CaN activity in cells, SH-SY5Y cells were transfected with NFAT-luciferase reporter plasmid (Stratagene, La Jolla, CA) and with the pmaxFP-Red-C-CaN constructs.

Twelve hours after transfection, cells were stimulated with 2 μM ionomycin and 100 nM PMA for 4 h. The cells were lysed in 100 μL of reporter lysis buffer (Promega, Madison, WI). Equivalent amounts of protein were measured using the luciferase assay system (Promega) in a luminescence counter (Perkin-Elmer). Expressions of the transfected RFP−CaN constructs were quantified by Western blot analysis using a standard curve obtained by blotting with different concentrations of recombinant CaN isoforms. Measured relative luminescence units (RLU) were normalized to the amount of additional expressed isoforms. As an internal standard, cells were transfected additionally with a β-galactosidase plasmid.

Elk-1 Reporter Gene Activity. CaN activity in cells were determined using the PathDetect Elk-1 *trans*-Reporting System (Stratagene). SH-SY5Y cells were transfected with the pmaxFP-Red-C-CaN constructs, the Elk-1 transactivator plasmid, the luciferase reporter plasmid, and the pFC-MEK1 plasmid. Since only the phosphorylated form of Elk-1 activates luciferase expression, CaN activity can be determined by measuring the decrease in luciferase activity. Twelve hours after transfection, cells were stimulated with

2 μM ionomycin for 4 h. Then, cells were lysed in 100 μL of reporter lysis buffer (Promega). Equivalent amounts of protein were measured using the luciferase assay substrate (Promega) in a luminescence counter (Perkin-Elmer). Expressions of the transfected RFP−CaN constructs were quantified by Western blot analysis. RLU were normalized to the amount of additional expressed CaN isoforms. As an internal standard, cells were transfected additionally with a β-galactosidase plasmid.

Confocal Laser Scanning Microscopy. SH-SY5Y cells transfected with the red fluorescent protein (RFP) fused with CaN isoforms were cultured on 10 mm coverslips. Cells were fixed in 4% paraformaldehyde with PBS for 30 min at room temperature. After being washed with PBS, the cells were permeabilized with 0.2% Triton X-100 in PBS containing 1% FCS for 5 min on ice and washed three times with PBS containing 1% FCS. Nuclei were stained with DAPI (BD Biosciences Pharmingen) for 10 min at room temperature and washed with PBS. Coverslips were mounted onto glass slides with Vectashield mounting medium H-1000 (Vector Laboratories Inc.). Cells were analyzed by confocal laser scanning microscopy (Nikon TE2000) at 750-fold magnification.

RESULTS

Expression of Human CaN Isoforms. Since other expression strategies lack CaN stability in the absence of the B subunit or suffer from the incomplete N-myristoylation of recombinant CaNB subunit, we expressed the three isoforms using a tandem expression construct according to the method of Mondragon et al. (*32*). To express CaNA β, CaNA γ, and CaNA β^{22-524}, an N-terminally truncated β isoform lacking the proline-rich sequence, the sequence of CaNA α was substituted with the other isoforms in the vector pET15b using restriction enzymes *Nde*I and *Xho*I. Because CaNB is myristoylated at its N-terminal glycine residue, the yeast *N*-myristoyltransferase was coexpressed in BL21(DE3) pLysE. Complete myristoylation of purified proteins was confirmed by Edman degradation revealing no N-terminal degradation (data not shown). The identity of the proteins was also verified by SDS−PAGE and tryptic digestion followed by mass spectroscopy. Proteins were purified to homogeneity using Ni^{2+}-NTA affinity chromatography and CaM-Sepharose chromatography (Figure 1). Western blot analysis of the different isoforms revealed an equimolar ratio of CaNA and -B. Accordingly, the addition of recombinant CaNB did not increase CaN activity in the performed activity assays.

Correct folding of CaN isoforms was verified by CD spectroscopy. The CD spectra of the purified CaN isoforms exhibit local minima at 208 and 222 nm, indicating a regular fold with a high α-helical content. Thereby, the three isoforms exhibit similarly shaped CD spectra (Figure S1 of the Supporting Information). However, the γ isoform shows an increased melting point of thermal denaturation when compared with the α and β isoforms, indicating a higher thermal stability (data not shown).

To further characterize the CaN isoforms, we measured the activating effect of CaM on phosphatase activity using pNPP and RII peptide as substrates. In these experiments, CaM activated the α isoform with the highest factor, whereas CaN β and γ exhibit weaker activations. These differences

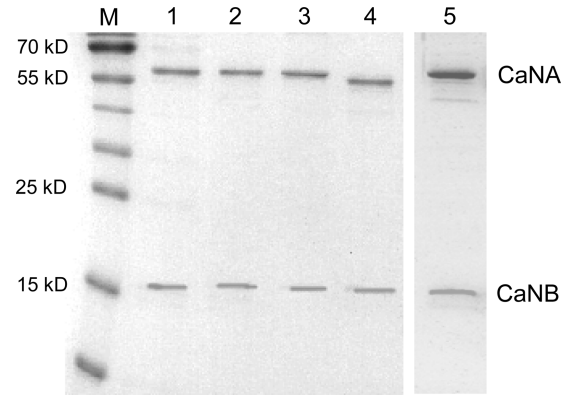

FIGURE 1: SDS−PAGE of purified myristoylated CaN heterodimers containing different isoforms of the catalytic subunit. CaN heterodimers were overexpressed with the *N*-myristoyltransferase in *Escherichia coli* BL21 pLysE cells and purified as described in Materials and Methods. Coomassie staining of SDS−PAGE gel shows the purified heterodimeric CaN isoforms CaN α (lane 1), CaN β (lane 2), CaN γ (lane 3), CaN β^{22-524} (lane 4), and CaN $\beta^{P14G/P18G}$ (lane 5).

are not a result of degradation of the C-terminal autoinhibitory domain of the CaNA subunits, since all three isoforms bind CaM-Sepharose with similar affinity, and moreover, intact C-termini were identified by tryptic digestion followed by mass spectrometry and SDS−PAGE.

Expression Patterns of Human CaNA Isoforms. Knockout experiments in mice revealed distinct physiological functions of CaNA α and β proposing that the isoforms either possess different substrate specificities and distinct regulatory mechanisms or exhibit different tissue and subcellular distributions (*24, 25*). To test whether the distinct cellular functions of the CaN isoforms are determined by different subcellular distributions, SH-SY5Y neuroblastoma cells were transfected with RFP fusion proteins of CaN isoforms and localization was analyzed by confocal fluorescence microscopy. As shown in Figure 2, cells transfected with the vector control exhibited equal staining throughout the cells, whereas all three isoforms displayed a predominant localization in the cytoplasm (Figure 2). These results indicate that distinct physiological functions of CaN isoforms are not conferred by differential subcellular localizations.

To study protein expression patterns, Western blot analysis using CaNA isoform-specific antibodies was performed. To control the specificities of the CaN antibodies, Western blots were performed using purified proteins demonstrating no cross reactivities of the applied antibodies (Figure S2 of the Supporting Information). The investigation of protein expression patterns of the CaN isoforms revealed that all isoforms are expressed in each tested cell line. However, analysis showed that the γ isoform is expressed in significantly smaller amounts when compared to the other two isoforms. For example, the γ isoform is expressed in ~20-fold smaller amounts in the human neuroblastoma SH-SY5Y cell line than the α isoform. The largest amounts of CaNA γ were observed in HeLa and MCF-7 cells. The CaNA α isoform is expressed at its highest levels in HeLa cells, whereas the β isoform is expressed at its highest levels in HEK 293 cells and in the human breast cancer MCF-7 cells. The comparison of expression levels showed that the CaNA α isoform is the predominantly expressed isoform in SH-SY5Y, HeLa, and A431 cells. Moreover, Western blot analysis showed that

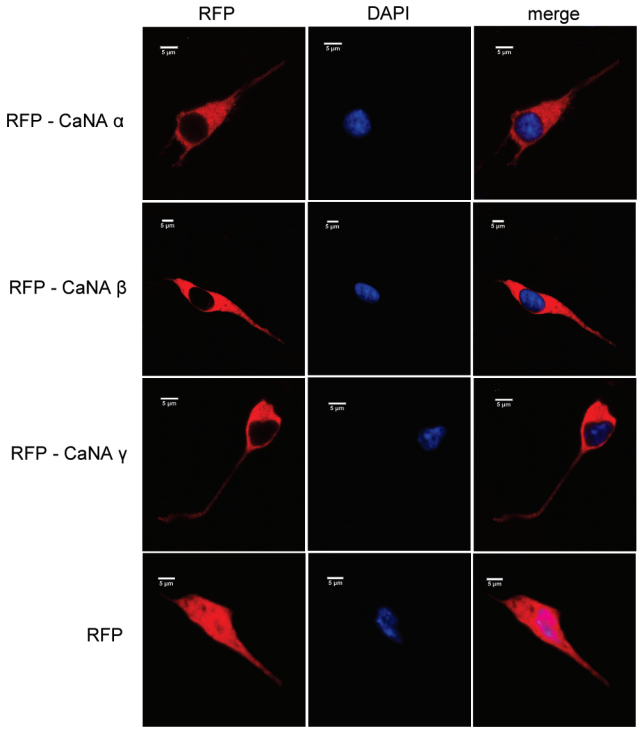

FIGURE 2: Subcellular distribution of the CaNA isoforms in SH-SY5Y neuroblastoma cells. The vectors expressing RFP fusion proteins of the isoforms of CaNA were transfected into SH-SY5Y cells, and subcellular localization was analyzed by confocal laser scanning microscopy. Nuclei were stained with DAPI. The three CaNA isoforms (α, *β*, and *γ*) exhibit a cytoplasmic subcellular distribution, whereas the RF protein is ubiquitously localized in neuroblastoma cells.

both the CaNA α and *β* isoforms are expressed in comparable amounts in Jurkat, Y79, and HEK 293 cells (Figure 3).

Substrate Specificities of CaN α, β, and γ. So far, no comparative analysis of substrate specificities of human CaN isoforms exists. Therefore, we studied substrate preferences of the three isoforms using various physiological CaN substrates. To enzymatically characterize the three CaN isoforms, we determined the kinetic constants of CaN-catalyzed dephosphorylation for RII peptide, DARPP-32, Elk-1, NFAT, and microtubule-associated protein Tau (Figure 4 and Tables 1 and 2).

Therefore, CaN substrates were labeled with ^{33}P and the respective protein kinase. Dephosphorylation reactions were assessed in the presence of various substrate concentrations, and kinetic parameters were analyzed by Lineweaver−Burk and Cornish−Bowden plots. Additionally, we studied the dephosphorylation of the small artificial substrate pNPP, which has been widely used to characterize phosphatase activity.

Our measurements revealed that the CaN holoenzyme that contains the α isoform of the catalytic subunit has a significantly higher catalytic efficiency in the case of Elk-1. The transcription factor is dephosphorylated with a 7-fold higher k_{cat}/K_m value by the α isoform when compared to the *β* isoform and a 2-fold higher catalytic efficiency when compared to CaN *γ*. Moreover, Tau is dephosphorylated 2-fold more efficiently by the α isoform when compared to the other two isoforms (Table 1). However, comparable catalytic efficiencies of CaN α and CaN *β* were observed in the case of the dephosphorylation of NFAT, RII peptide, and

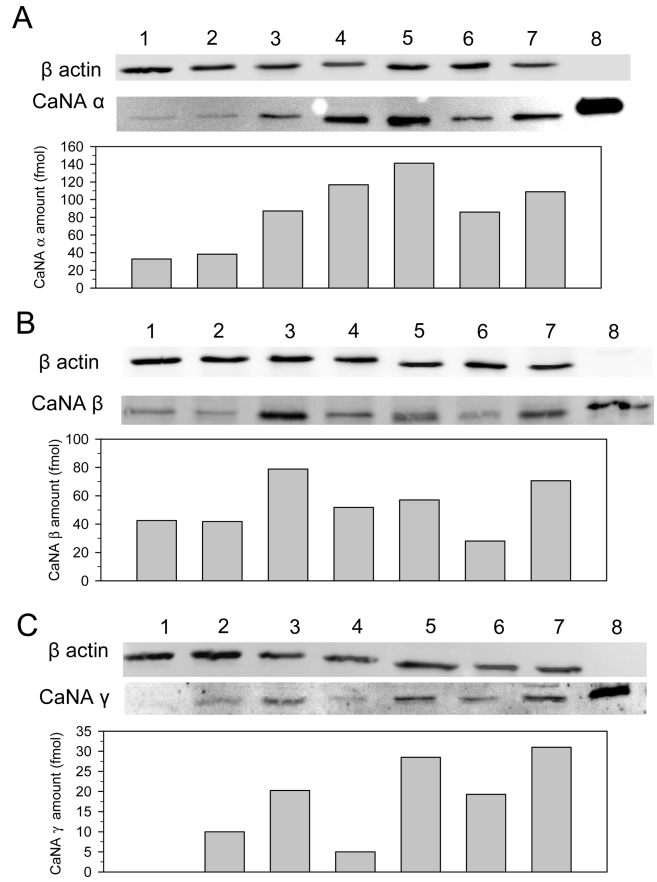

FIGURE 3: Distribution of the CaNA isoforms in different human cell lines. Fifteen microliters of 1 mg/mL cell lysate of the human cell lines (lane 1, Y79; lane 2, Jurkat; lane 3, HEK 293; lane 4, SH-SY5Y; lane 5, HeLa; lane 6, A431; lane 7, MCF-7; and lane 8, 0.5 pmol of recombinant CaN α, 0.05 pmol of CaN *β*, and 1 pmol of CaN *γ*) was applied on 15% SDS gels. Western blots were analyzed using specific antibodies against CaNA α (A), CaNA *β* (B), and CaNA *γ* (C). Analysis with anti-*β*-actin antibody was performed to confirm equal loading of the protein samples. The blots were quantified using densitometry software, and data were normalized to *β*-actin. Amounts of CaNA in the cell lines were calculated using purified CaNA isoforms as standards.

pNPP, whereas the *γ* isoform displays significantly lower efficiencies for these substrates. In contrast, CaN *γ* represents the best DARPP-32 phosphatase, exhibiting a 2-fold higher k_{cat}/K_m value in the case of DARPP-32 and Elk-1 when compared to the CaN *β* isoform.

To determine the contribution of the distinct CaN isoforms to substrate dephosphorylation in a cellular system, NFAT and Elk-1 reporter gene activity was measured in RFP−CaN transfected SH-SY5Y cells (Figure 5). As shown in Figure 5A, Elk-1 reporter gene activity was decreased to ∼50% when cells were transfected with CaNA α, whereas CaNA *β* inhibited reporter gene activity to only 80% of the vector control. In accordance with the determined catalytic constants, CaNA *γ* dephosphorylated Elk-1 more efficiently than CaNA *β* as shown by a significantly lower luciferase activity. In addition, the CaN isoform-mediated increase in NFAT reporter gene activity corresponds well with the order of the measured catalytic efficiencies toward NFAT (Figure 5B). CaNA α-transfected cells exhibited the greatest increase in luciferase activity followed by CaNA *β*-transfected cells. In contrast, additional expression of CaNA *γ* did not affect NFAT activity in SH-SY5Y cells.

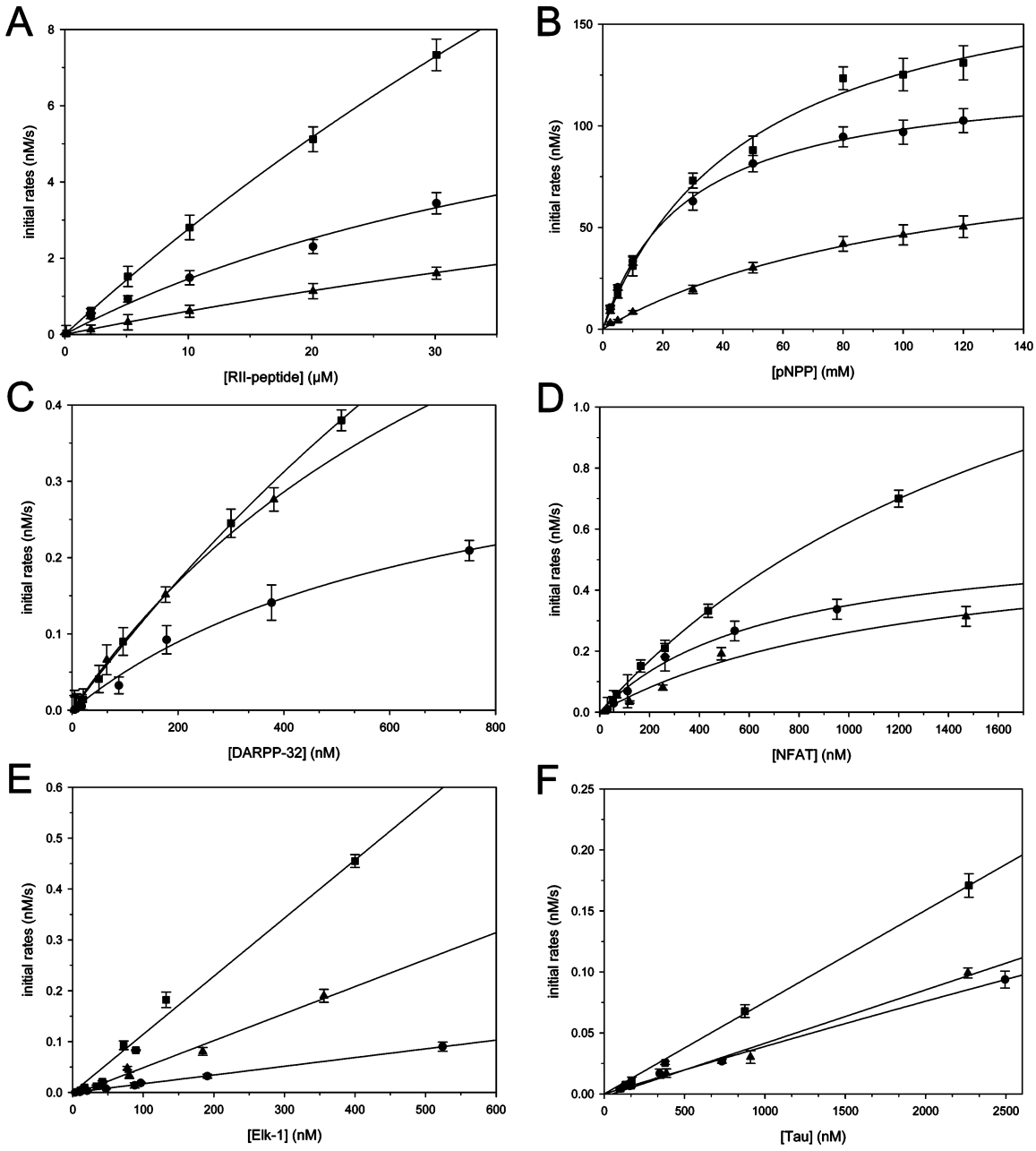

FIGURE 4: Michaelis−Menten plots of CaN α, β, and γ using different substrates. (A) In the RII peptide assay, the kinetic constants were determined with 15 nM CaN α (■), CaN β (●), or CaN γ (▲) and 150 nM CaM. After addition of 0−30 μM PKA-phosphorylated nonbiotinylated RII peptide and 0.1 μM biotinylated ^{33}P-labeled RII peptide, the samples were incubated for 1 h at 30 °C. CaN activity was determined by measuring biotinylated ^{33}P-labeled RII peptide bound to a streptavidin-coated scintillation plate using a MicroBeta counter. (B) In the pNPP assay, 37 nM CaN α (■), CaN β (●), and CaN γ (▲) were measured in the presence of pNPP concentrations ranging from 0 to 120 mM. The time course of 4-nitrophenolate release was measured at 405 nm for 30 min. Initial rates were determined by linear regression. (C) Kinetic constants for the dephosphorylation of DARPP-32 by CaN isoforms were measured using 9 nM CaN α (■), CaN β (●), or CaN γ (▲) and 150 nM CaM. After addition of 0−800 nM DARPP-32 and a reaction time between 5 and 40 min at 30 °C, proteins were precipitated by adding 10 mg/mL BSA and 20 μL of 20% TCA. Samples were centrifuged for 15 min at 15000*g*, and the amount of supernatant was measured by liquid scintillation counting. (D) Measurements of the dephosphorylation of NFAT by CaN isoforms were performed using 9 nM CaN α (■), CaN β (●), or CaN γ (▲) and 150 nM CaM. Dephosphorylation was started by addition of 0−1500 nM NFAT, and reaction mixtures were incubated for 3−60 min at 30 °C. Then, proteins were precipitated by adding 10 mg/mL BSA and 20 μL of 20% TCA followed by centrifugation for 15 min at 15000*g*. The amount of released ^{33}P was measured by liquid scintillation counting. (E) Determinations of kinetic constants for dephosphorylation of Elk-1 by CaN isoforms were performed using 30 nM CaN α (■), CaN β (●), or CaN γ (▲) and 150 nM CaM. After addition of 0−530 nM Elk-1 and incubation for 2−40 min at 30 °C, proteins were precipitated by adding 10 mg/mL BSA and 20 μL of 20% TCA. Subsequently, samples were centrifuged for 15 min at 15000*g*, and the amount of supernatant was measured by liquid scintillation counting. (F) Kinetic constants of Tau dephosphorylation by different CaN isoforms were measured using 70 nM CaN α (■), CaN β (●), or CaN γ (▲) and 150 nM CaM. Reaction was started by addition of 0−2500 nM Tau followed by incubation for 3−90 min at 30 °C. Then, protein was precipitated by adding 10 mg/mL BSA and 20 μL of 20% TCA. Subsequently, samples were centrifuged for 15 min at 15000*g*, and the amount of supernatant was measured by liquid scintillation counting. Each value is the mean of triplicate determinations with a standard deviation of ≤10%.

The determination of k_{cat} and K_m values revealed that even though the catalytic efficiencies of CaN α and CaN β are nearly identical in most cases both the k_{cat} and K_m values differ greatly between the two isoforms (Table 2). Thus,

Table 1: Catalytic Efficiencies of CaN Heterodimers Comprising the α, β, β^{22-524}, and γ Isoforms of the Catalytic Subunit and the Regulatory Subunit B1 for Different Substrates[a]

	k_{cat}/K_m (mM^{-1} s^{-1})					
	pNPP	RII	NFAT	Elk-1	DARPP-32	Tau
CaN α	0.108	19.7	55.1	38.9	104	1.08
CaN β	0.111	18.0	52.1	5.87	60.3	0.69
CaN β^{22-524}	0.18	16.7	67.9	not determined	76.6	not determined
CaN γ	0.042	3.55	15.7	18.3	109	0.61

[a] Each value is the mean of triplicate determinations with a standard deviation of <5%.

kinetic data showed that CaN α possesses for all analyzed protein substrates the highest k_{cat} value, whereas the β isoforms exhibits in all cases the lowest K_m value. The higher apparent substrate affinity and the lower turnover number of the CaN β may indicate the existence of an additional regulatory motif of these isoforms. The catalytic subunits of the three human CaN isoforms differ, especially in the N- and C-termini and the loops between the functional domains. For example, the β isoforms contain a proline-rich sequence at the N-terminus that may represent a protein−protein interaction motif conferring the higher substrate affinity (Figure 6). To investigate the hypothesis, we cloned and expressed the CaN β^{22-524} construct lacking the proline-rich N-terminus.

Biochemical Characterization of CaN β Variants. The CaN β isoform lacking the proline-rich N-terminus, CaN β^{22-524}, was cloned into the pET15b vector and purified to homogeneity using Ni^{2+}-NTA affinity chromatography and CaM-Sepharose chromatography (Figure 1). The identity of the protein was verified by SDS−PAGE and tryptic digestion followed by mass spectroscopy. Far-UV CD spectra revealed that CaN β^{22-524} and CaN β exhibit a similar fold and midpoints of thermal denaturation (Figure S1 of the Supporting Information). Moreover, both proteins were activated by CaM to the same extent, also indicating comparable folds of both proteins (Figure S3 of the Supporting Information). Addition of recombinant B subunit to the purified CaN β and CaN β^{22-524} heterodimers did not change phosphatase activity, indicating that the N-terminus has no influence on the correct formation of both CaN β holoenzymes. Expression of the RFP−CaNA β^{22-524} fusion protein in SH-SY5Y cells showed a predominant expression in the cytosol as observed for the wild-type protein and the other two isoforms, proposing that the N-terminus may determine different substrate affinities and not the subcellular distribution of the protein (Figure 7).

To investigate whether the proline-rich N-terminus determines the high substrate affinity and low turnover numbers of CaN β when compared with those of the α isoform, we measured kinetic constants for the dephosphorylation of NFAT, DARPP-32, RII peptide, and pNPP (Table 3 and Figure S4 of the Supporting Information). These measurements revealed that CaN β^{22-524} exhibits a catalytic efficiency comparable to that of CaN β when RII peptide was used as the substrate. However, the substrate affinity of the N-terminally truncated CaN β isoform was 7-fold decreased, whereas the k_{cat} value was increased to the same extent. A similar effect of CaN β truncation was observed with DARPP-32 as the substrate, showing a 10-fold increase in K_m and a 13-fold increase in k_{cat}. The analysis of CaN β-mediated NFAT dephosphorylation revealed a slightly increased catalytic efficiency of the truncated form. In this case, the K_m value of CaN β^{22-524} was also significantly increased and the turnover number was elevated. Interestingly, the catalytic constants of the truncated CaN β isoform correspond well with the k_{cat} and K_m values obtained with the CaN α isoform, indicating that the proline-rich sequence may represent an additional protein−protein interaction motif and therefore determines the higher substrate affinity of CaN β. To investigate whether a well-defined structure of the polyproline motif mediates the unique catalytic properties of the β isoform, two mutations of Pro to Gly in the middle of the polyproline sequence at positions 14 and 18 were introduced. Mutations of Pro to Gly were chosen to disrupt the structure of a possible polyproline II helix. The characterization of the CaN $\beta^{P14G/P18G}$ mutant using far-UV CD spectroscopy revealed a similar secondary structure content when compared with that of wild-type CaN β and the N-terminally truncated form of CaN β^{22-524}, indicating correct folding of the protein (Figure S1 of the Supporting Information). The determination of Michaelis−Menten constants using the RII peptide revealed a K_m value of 102 μM and a k_{cat} value of 1.28 s^{-1}, whereas the catalytic efficiency of the CaN $\beta^{P14G/P18G}$ mutant is decreased 1.5-fold when compared with that of the wild-type protein (Figure S4 of the Supporting Information). Thus, the CaN $\beta^{P14G/P18G}$ mutant exhibits catalytic constants that more resemble the values obtained with CaN β^{22-524} than those of the wild-type protein.

In contrast to the significant decrease in substrate affinity of CaN β^{22-524} for proteinaceous substrates, the truncated isoform exhibits a nearly identical K_m value for the small artificial substrate pNPP. The k_{cat}/K_m value for pNPP is increased in case of the truncated β isoforms due to an almost 2-fold higher k_{cat} value, whereas the catalytic efficiencies of CaN β^{22-524} for RII peptide, NFAT, and DARPP-32 correspond well with those of the full-length protein.

DISCUSSION

The human genome encodes three distinct CaNA isoforms (α, β, and γ), whose specific functions and properties are less understood, so far. Now, our comparative study provides evidence that the distinct CaN isoforms exhibit differences in substrate specificity, even though all three isoforms are able to dephosphorylate the same set of substrates. For example, transcription factor Elk-1 is dephosphorylated 7-fold more efficiently by the α isoform than by the CaN β isoform. Elk-1 initiates the transcription of growth factor inducible genes following phosphorylation of serine 383 by MAP kinases (*34*−*36*). Thus, through CaN catalyzed dephosphorylation of Elk-1, Ca^{2+} has a negative effect on the expression of Elk-1 target genes (*17*). The preference of CaNA α for Elk-1 was confirmed by Elk-1 reporter gene activity measurements, as well. Thus, our results propose that in tissues where CaN β is the predominant expressed isoform the influence of an increase in the cytosolic concentration of Ca^{2+} on Elk-1-mediated transcriptional activity is less potent, indicating that substrate selectivity and expression patterns of CaN isoforms also determine Ca^{2+}-triggered gene expression.

The CaN α isoform is also the predominant Tau phosphatase dephosphorylating the microtubule-associated protein

Table 2: Comparison of the K_m and k_{cat} Values of CaN α, β, β^{22-524}, and γ toward Different Substrates[a]

	pNPP		RII		NFAT		DARPP-32	
	K_m (μM)	k_{cat} (s^{-1})	K_m (μM)	k_{cat} (s^{-1})	K_m (μM)	k_{cat} (s^{-1})	K_m (μM)	k_{cat} (s^{-1})
CaN α	39600	4.32	136	2.76	2.04	0.11	2.22	0.23
CaN β	33300	3.75	16.3	0.32	0.69	0.04	0.70	0.04
CaN β^{22-524}	35200	6.31	125	2.18	2.62	0.25	6.90	0.54
CaN γ	117000	2.24	245	0.87	1.27	0.02	0.94	0.13

[a] Each value is the mean of triplicate determinations with a standard deviation of <5%.

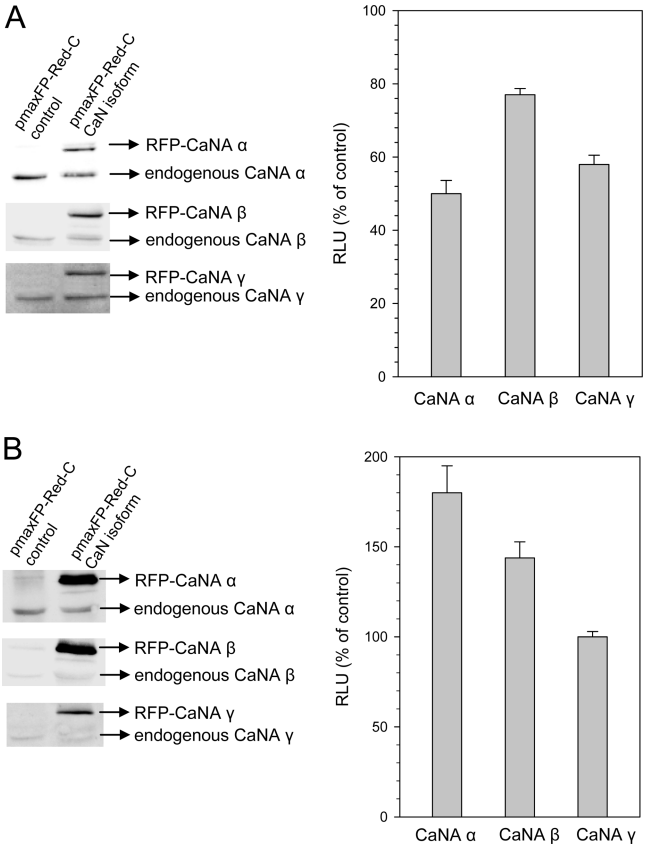

FIGURE 5: Effect of CaNA isoforms on NFAT and Elk-1 reporter gene activity. (A) SH-SY5Y cells were transfected with the pmaxFP-Red-C-CaN constructs, the Elk-1 transactivator plasmid, and the luciferase reporter plasmid. To increase Elk-1 reporter gene activity, cells were transfected additionally with the pFC-MEK1 plasmid. The CaN-mediated decrease in Elk-1 reporter gene activity was measured after incubation for 4 h with ionomycin. Moreover, Western blotting with CaN isoform-specific antibodies was performed to determine the amount of expressed RFP−CaN isoforms. Relative luminescence units (RLU) were represented as the percent of vector-transfected control after normalization of the reporter gene activity to the amount of additional expressed CaN isoforms. (B) SH-SY5Y cells were transfected with the pmaxFP-Red-C-CaN constructs and the NFAT-luciferase reporter plasmid. After incubation with 100 nM PMA and 2 μM ionomycin for 4 h, CaN-mediated NFAT activation was assessed using the luciferase assay system. To determine the amount of expressed RFP−CaN isoforms, Western blot analysis was performed using CaN isoform-specific antibodies. Relative luminescence units (RLU) were represented as the percent of vector-transfected control after normalization of the reporter gene activity to the amount of additional expressed CaN isoforms.

with a 2-fold higher catalytic efficiency in comparison with CaN β and γ. In this respect, it is noteworthy that Tau is hyperphosphorylated at serine 396 and serine 404 in CaN α knockout mice (*37*). Tau hyperphosphorylation is one of the major molecular hallmarks of Alzheimer's disease. The discrepancy between marked effects of CaN α deficiency in

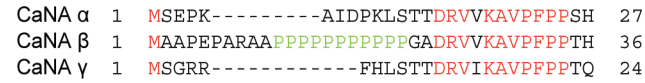

FIGURE 6: Amino acid sequence alignment of the N-terminal regions of the three CaNA isoforms. Sequence analysis revealed that CaNA α, β, and γ vary, especially in their N- and C-terminal regions. CaNA β contains a polyproline sequence at the N-terminus, which is not present in the other isoforms (green). Identical amino acids are colored red.

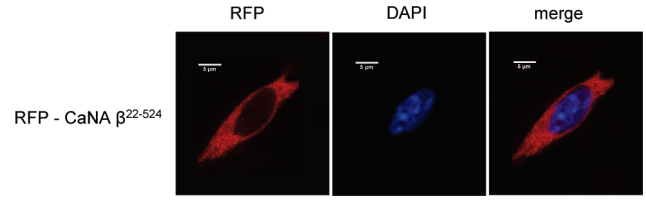

FIGURE 7: Subcellular localization of CaNA β^{22-524} in SH-SY5Y neuroblastoma cells. The RFP−CaNA β^{22-524} fusion protein was expressed in SH-SY5Y cells, and its subcellular distribution was analyzed by confocal laser scanning microscopy. Nuclei were visualized by DAPI staining. CaNA β^{22-524}, which lacks the proline-rich sequence of CaNA β, exhibited a cytoplasmic localization.

brain tissue and the relatively small differences in Tau dephosphorylation by CaN isoforms can be explained by the dephosphorylation of additional in vitro sites that are not preferentially recognized by the CaN α isoform. Moreover, CaNA α knockout mice revealed a negative effect on hippocampal depotentiation, while long-term depression and long-term potentiation (LTP) were unaffected (*37*). LTP depends on a synergistic mechanism involving phosphorylation of both cAMP response element binding protein (CREB) and DARPP-32 via activation of PKA. Our results showed similar catalytic efficiencies for DARPP-32 dephosphorylation by CaN α and γ, whereas CaN β exhibits a significantly lower DARPP-32 phosphatase activity. This result indicates that the γ isoforms may compensate for the loss of CaN α in the regulation of LTP. Additionally, reduced CaN γ expression levels in brains of schizophrenia patients was demonstrated, proposing an involvement of CaN γ in the pathogenesis of this disorder (*38*). Interestingly, abnormal signaling through dopaminergic pathways that is connected with altered DARPP-32 phosphorylation is also linked to schizophrenia (*39*). Therefore, decreased CaN activity may lead to schizophrenia by permanent DARPP-32 phosphorylation that results in PP1 inhibition and increased levels of expression of CREB-dependent genes.

In contrast to the proposed function of CaN γ in DARPP-32 dephosphorylation, the γ isoform possesses a significantly lower catalytic efficiency for NFAT, exhibiting a 3-fold lower k_{cat}/K_m value than CaN α and CaN β. Analysis of NFAT reporter gene activity of cells transfected with the different CaN isoforms also revealed significant substrate specificities. CaNA α dephosphorylated NFAT 1.5-fold more efficiently than CaNA β, whereas CaNA γ had no effect on NFAT

activity in the cellular system. The dephosphorylation of NFAT plays an important role in the antigen-specific immune response. Accordingly, the impaired antigen-specific immune response that originates from a defective stimulation-induced NFAT activation was observed in CaN $\alpha^{-/-}$ and CaN $\beta^{-/-}$ T cells (*24, 25*). Analysis of expression patterns of CaN isoforms implies an important function for CaN β in T cell development. CaN β was identified as the predominant isoform in T and B lymphocytes, spleen, and thymus compared to the α isoform (*25, 40*). In connection with our activity measurements, these data indicate a prominent role for CaN α and β in NFAT-mediated T cell development. In contrast, there is no evidence of CaN γ function in NFAT signaling.

Even though catalytic domains of CaN isoforms display a high degree of sequence identity, our results revealed substrate preferences of the isoforms that may contribute to distinct physiological functions. The differences in substrate recognition may possibly result from additional substrate binding motifs outside the catalytic sites. Such CaN binding sites were already identified for NFAT and certain other CaN-interacting proteins (*41, 42*). For example, the NFAT transcription factor family contains two CaN binding sites with the consensus sequence PxIxIT and LxVP that confer different CaN binding affinities among the NFATs. Both interaction sites were recently identified in the sequences for multiple other proteins like the neuronal A-kinase anchoring protein AKAP79, the African swine fever virus protein A238L, the human T cell leukemia/lymphotropic virus type I $p12^{I}$ protein, and the yeast proteins Crz1p and Slm1p. However, there are reports showing no strict requirement for the exact CaN consensus binding motive. The human K^+ channel TRESK that contains the modified interaction motif PQIVID binds to CaN with high affinity as well, exhibiting a K_i value of 10 μM (*43*). Interestingly, a motif (^{408}PSISVD^{413}) very similar to that of TRESK and NFATc3 (PSIQIT) can be found close to the phosphorylation site Ser389 in the transcription factor Elk-1 (Figure S5 of the Supporting Information). Moreover, DARPP-32 contains the sequence ^{10}QFSVPAP^{16} within the N-terminal region that is very similar to the second CaN binding site in NFAT (QFLSVPSP). Thus, it is possible that substrate specificities of CaN isoforms may result from different binding affinities for the additional interaction motifs.

Fluorescence confocal microscopy experiments demonstrated that all three isoforms display the same cytoplasmic distribution, indicating that specific functions of CaNA isoforms are determined by different substrate specificities in the cell with comparable expression levels. To obtain further indications for specific functions of the three isoforms, we analyzed CaNA expression patterns in different cell lines. These experiments revealed that not only CaNA α and CaNA β but also the γ isoform is expressed in all tested cell lines. The CaNA γ isoform was originally described exclusively as a testis-specific form. Additionally, it was thought that CaNA γ interacts with a testis-specific isoform of the regulatory subunit, CaNB 2 (*44, 45*). However, our coexpression experiments with the CaNA γ catalytic isoform with both regulatory isoforms revealed that only the ubiquitously expressed CaNB 1 forms active dimers with the γ isoform. These results correspond well with previous findings showing that CaN γ protein in mouse brain forms complexes with CaNB 1 (*46*). Besides CaNA γ protein expression in brain and testis, the protein was identified in kidney, as well (*47*). Additionally, mRNA expression of CaNA γ was shown in all human tissues (*46*). Our experiments revealed that the γ isoform is expressed in all tested cell lines, including neuroblastoma, kidney, breast, epithelial, and cervical carcinoma derived cell lines. However, the CaNA γ isoform is expressed to significantly lower levels when compared to the other two isoforms. CaNA α is the predominant isoform in SH-SY5Y, HeLa, MCF-7, and A431 cells, whereas CaNA β exhibits the highest concentrations in Y79, Jurkat, and HEK 293 cells. These results agree well with described tissue distributions of the α and β isoforms, demonstrating high levels of CaN α in brain, while CaN β was identified as the predominant isoform in T and B cells, spleen, and thymus (*25, 40, 48, 49*). In kidney, CaN α is exclusively expressed in tubules, whereas CaN β staining was found in the glomerular region, suggesting that both isoforms may possess different functions (*40*).

Kinetic analysis of CaN-mediated dephosphorylation of different substrates revealed differences not only in the substrate specificities but also in the k_{cat} and K_m values. Thus, even though CaN α and CaN β show similar catalytic efficiencies for NFAT and RII peptide, they differ greatly in their binding affinities and turnover numbers. The β isoform exhibits for all kinetically analyzed substrates significantly higher binding affinities than the α and γ isoforms. CaN β exhibits a 3-fold lower K_m value in the case of NFAT and DARPP-32, and even a 7-fold higher affinity for the RII peptide when compared to the α isoform. In comparison to CaN γ, CaN β exhibits an even 15-fold higher substrate affinity for the RII peptide and a 2-fold lower K_m value in the case of NFAT. Additionally, measurements revealed a significantly lower turnover number for CaN β compared to those of the other isoforms for all analyzed proteinaceous substrates, despite NFAT. However, no significant differences in catalytic constants were observed between the CaN α and CaN β isoforms when the small substrate pNPP was used, indicating that secondary binding sites of CaN are involved in protein substrate recognition. Sequence analysis shows that the catalytic domains of the three isoforms are highly conserved, whereas the N-terminus of the β isoform displays a unique structural feature among the isoforms. The N-terminus of CaN β contains a sequence of 11 consecutive proline residues. Data regarding the structure of the N-terminus are still lacking because only the α isoform has been crystallized, so far. However, molecular modeling indicates the existence of an 11-residue type II polyproline helix (*31*). Polyproline motifs were found in a multitude of proteins where they possess important functions in signal transduction events, cell migration, transcription, and immune response. Moreover, polyproline motifs constitute recognition motifs for protein−protein interactions. For example, SH3, WW, and several new interaction domains prefer proline-rich ligand sequences (*50*). To investigate whether the proline-rich N-terminus confers the comparatively high protein substrate affinities among the CaN isoforms, we analyzed kinetic parameters of a CaN β variant lacking the proline-rich sequence. These measurements revealed that CaN β^{22-524} exhibits significantly lower substrate binding affinities and increased turnover numbers for the three analyzed substrates when compared to the full-

length protein. In contrast, the specificity constants k_{cat}/K_m of CaN β variants differ only slightly, indicating that the substrate specificity is not influenced by the proline-rich N-terminus. Interestingly, the truncated CaN β variant shows similar substrate affinities and k_{cat} values in comparison to the CaN α isoform. In the case of the small artificial substrate pNPP, truncated CaN β and full-length CaN β exhibit similar K_m values, suggesting that the proline-rich sequence contributes only to the interaction with protein substrates. To determine whether the proline-rich motif forms a polyproline II helix, two glycine residues were introduced into the polyproline sequence to disrupt the putative secondary structure. The resulting CaN $\beta^{P14G/P18G}$ mutant revealed a 6-fold increased K_m value and a 4-fold higher k_{cat} value that correspond well with the constants observed with the N-terminally truncated variant, indicating that the formation of a well-defined secondary structure of the N-terminal polyproline determines the catalytic properties of the isoform.

The molecular mechanism of how the proline-rich sequence influences kinetic constants is still enigmatic, since the N-terminus of the catalytic subunit in the crystal structure of CaN α exhibits no contacts with the active site and substrate binding region (*51*). However, X-ray structure analysis showed that the N-terminus of one CaNA interacts with the active site residues of a second CaNA in the crystallographic asymmetric unit. The question of whether these observations are biologically relevant or only the consequence of the crystal packing remains to be answered.

Molecular modeling suggested that an 11-residue type II polyproline helix exactly spans the length of the central helix of CaM and led to the proposal that the N-terminus of CaN β may affect CaM binding (*52*). However, our activity measurements indicate that truncated CaN β and full-length CaN β exhibit similar binding affinities for CaM. Another study suggested that the polyproline helix may instead interfere with the binding of the regulatory B subunit and thus may lead to differences in kinetic constants (*31*). Interestingly, the crystal structure revealed considerable contacts of the CaN α N-terminus with Ca^{2+} binding motif 3 of the B subunit, suggesting a role in CaNB binding and thus regulation of phosphatase activity. Additionally, it was proposed that the formation of a salt bridge between Glu53 of CaNA α and Lys134 of CaNB contributes to a conformational change in the catalytic subunit leading to the activation of CaN (*53*). The loss of phosphatase activity after proteolytic removal of the CaN α N-terminus also suggests an involvement in the regulation of the active site (*19*). Thus, the extended proline-rich N-terminus of CaNA β may mediate additional contacts with the regulatory subunit, thereby influencing the conformation of the active site and changing the catalytic constants of the phosphatase. In this regard, it is notable that binding of CaNB and binding of the polyproline motif have similar effects on the catalytic properties of CaN, leading to increased substrate affinities. However, as long as the structure of CaN β is lacking, the mechanism of direct modulation of substrate binding by the N-terminus of CaN β cannot be finally explained.

ACKNOWLEDGMENT

Mouse Tau A was kindly provided by Prof. Dr. Eckhard Mandelkow (Hamburg, Germany). The tandem expression construct CaNA α and CaNB 1 in pET15a as well as the *N*-myristoyltransferase were a gift of J. O. Liu (Baltimore, MD).

SUPPORTING INFORMATION AVAILABLE

CD spectra showing the correct folding of the calcineurin isoforms and additional data concerning the kinetic characterization of the isoforms and the isoform specificity of the antibodies. This material is available free of charge via the Internet at http://pubs.acs.org.

REFERENCES

1. Clipstone, N. A., and Crabtree, G. R. (1992) Identification of calcineurin as a key signalling enzyme in T-lymphocyte activation. *Nature 357*, 695–697.
2. Taigen, T., De Windt, L. J., Lim, H. W., and Molkentin, J. D. (2000) Targeted inhibition of calcineurin prevents agonist-induced cardiomyocyte hypertrophy. *Proc. Natl. Acad. Sci. U.S.A. 97*, 1196–1201.
3. Tong, G., Shepherd, D., and Jahr, C. E. (1995) Synaptic desensitization of NMDA receptors by calcineurin. *Science 267*, 1510–1512.
4. Mansuy, I. M., Mayford, M., Jacob, B., Kandel, E. R., and Bach, M. E. (1998) Restricted and regulated overexpression reveals calcineurin as a key component in the transition from short-term to long-term memory. *Cell 92*, 39–49.
5. Lautermilch, N. J., and Spitzer, N. C. (2000) Regulation of calcineurin by growth cone calcium waves controls neurite extension. *J. Neurosci. 20*, 315–325.
6. Nichols, R. A., Suplick, G. R., and Brown, J. M. (1994) Calcineurin-mediated protein dephosphorylation in brain nerve terminals regulates the release of glutamate. *J. Biol. Chem. 269*, 23817–23823.
7. Hemmings, H. C., Jr., Greengard, P., Tung, H. Y., and Cohen, P. (1984) DARPP-32, a dopamine-regulated neuronal phosphoprotein, is a potent inhibitor of protein phosphatase-1. *Nature 310*, 503–505.
8. Lian, Q., Ladner, C. J., Magnuson, D., and Lee, J. M. (2001) Selective changes of calcineurin (protein phosphatase 2B) activity in Alzheimer's disease cerebral cortex. *Exp. Neurol. 167*, 158–165.
9. Mandelkow, E. M., and Mandelkow, E. (1998) Tau in Alzheimer's disease. *Trends Cell Biol. 8*, 425–427.
10. Casolaro, V., Georas, S. N., Song, Z., and Ono, S. J. (1996) Biology and genetics of atopic disease. *Curr. Opin. Immunol. 8*, 796–803.
11. Goldfeld, A. E., Tsai, E., Kincaid, R., Belshaw, P. J., Schrieber, S. L., Strominger, J. L., and Rao, A. (1994) Calcineurin mediates human tumor necrosis factor α gene induction in stimulated T and B cells. *J. Exp. Med. 180*, 763–768.
12. Jain, J., Loh, C., and Rao, A. (1995) Transcriptional regulation of the IL-2 gene. *Curr. Opin. Immunol. 7*, 333–342.
13. McCaffrey, P. G., Kim, P. K., Valge-Archer, V. E., Sen, R., and Rao, A. (1994) Cyclosporin A sensitivity of the NF-κB site of the IL2R α promoter in untransformed murine T cells. *Nucleic Acids Res. 22*, 2134–2142.
14. Rao, A., Luo, C., and Hogan, P. G. (1997) Transcription factors of the NFAT family: Regulation and function. *Annu. Rev. Immunol. 15*, 707–747.
15. Tocci, M. J., Matkovich, D. A., Collier, K. A., Kwok, P., Dumont, F., Lin, S., Degudicibus, S., Siekierka, J. J., Chin, J., and Hutchinson, N. I. (1989) The immunosuppressant FK506 selectively inhibits expression of early T cell activation genes. *J. Immunol. 143*, 718–726.
16. Liu, J., Farmer, J. D., Jr., Lane, W. S., Friedman, J., Weissman, I., and Schreiber, S. L. (1991) Calcineurin is a common target of cyclophilin-cyclosporin A and FKBP-FK506 complexes. *Cell 66*, 807–815.
17. Sugimoto, T., Stewart, S., and Guan, K. L. (1997) The calcium/calmodulin-dependent protein phosphatase calcineurin is the major Elk-1 phosphatase. *J. Biol. Chem. 272*, 29415–29418.
18. Sharma, R. K., Desai, R., Waisman, D. M., and Wang, J. H. (1979) Purification and subunit structure of bovine brain modulator binding protein. *J. Biol. Chem. 254*, 4276–4282.

19. Hubbard, M. J., and Klee, C. B. (1989) Functional domain structure of calcineurin A: Mapping by limited proteolysis. *Biochemistry 28*, 1868–1874.
20. Aitken, A., Klee, C. B., and Cohen, P. (1984) The structure of the B subunit of calcineurin. *Eur. J. Biochem. 139*, 663–671.
21. Gerber, D. J., Hall, D., Miyakawa, T., Demars, S., Gogos, J. A., Karayiorgou, M., and Tonegawa, S. (2003) Evidence for association of schizophrenia with genetic variation in the 8p21.3 gene, PPP3CC, encoding the calcineurin γ subunit. *Proc. Natl. Acad. Sci. U.S.A. 100*, 8993–8998.
22. Liu, Y. L., Fann, C. S., Liu, C. M., Chang, C. C., Yang, W. C., Hung, S. I., Yu, S. L., Hwang, T. J., Hsieh, M. H., Liu, C. C., Tsuang, M. M., Wu, J. Y., Jou, Y. S., Faraone, S. V., Tsuang, M. T., Chen, W. J., and Hwu, H. G. (2007) More evidence supports the association of PPP3CC with schizophrenia. *Mol. Psychiatry 12*, 966–974.
23. Mathieu, F., Miot, S., Etain, B., El Khoury, M.-A., Chevalier, F., Bellivier, F., Leboyer, M., Giros, B., and Tzavara, E. T. (2008) Association between the PPP3CC gene, coding for the calcineurin gamma catalytic subunit, and bipolar disorder. *Behav. Brain Funct. 4*, paper 2.
24. Zhang, B. W., Zimmer, G., Chen, J., Ladd, D., Li, E., Alt, F. W., Wiederrecht, G., Cryan, J., O'Neill, E. A., Seidman, C. E., Abbas, A. K., and Seidman, J. G. (1996) T cell responses in calcineurin A α-deficient mice. *J. Exp. Med. 183*, 413–420.
25. Bueno, O. F., Brandt, E. B., Rothenberg, M. E., and Molkentin, J. D. (2002) Defective T cell development and function in calcineurin A β-deficient mice. *Proc. Natl. Acad. Sci. U.S.A. 99*, 9398–9403.
26. Zhuo, M., Zhang, W., Son, H., Mansuy, I., Sobel, R. A., Seidman, J., and Kandel, E. R. (1999) A selective role of calcineurin Aα in synaptic depotentiation in hippocampus. *Proc. Natl. Acad. Sci. U.S.A. 96*, 4650–4655.
27. Gooch, J. L., Toro, J. J., Guler, R. L., and Barnes, J. L. (2004) Calcineurin A-α but not A-β is required for normal kidney development and function. *Am. J. Pathol. 165*, 1755–1765.
28. Bueno, O. F., Wilkins, B. J., Tymitz, K. M., Glascock, B. J., Kimball, T. F., Lorenz, J. N., and Molkentin, J. D. (2002) Impaired cardiac hypertrophic response in calcineurin A β-deficient mice. *Proc. Natl. Acad. Sci. U.S.A. 99*, 4586–4591.
29. Gooch, J. L. (2006) An emerging role for calcineurin Aα in the development and function of the kidney. *Am. J. Physiol. 290*, 769–776.
30. Cubellis, M. V., Caillez, F., Blundell, T. L., and Lovell, S. C. (2005) Properties of polyproline II, a secondary structure element implicated in protein-protein interactions. *Proteins 58*, 880–892.
31. Perrino, B. A., Wilson, A. J., Ellison, P., and Clapp, L. H. (2002) Substrate selectivity and sensitivity to inhibition by FK506 and cyclosporin A of calcineurin heterodimers composed of the α or β catalytic subunit. *Eur. J. Biochem. 269*, 3540–3548.
32. Mondragon, A., Griffith, E. C., Sun, L., Xiong, F., Armstrong, C., and Liu, J. O. (1997) Overexpression and purification of human calcineurin α from *Escherichia coli* and assessment of catalytic functions of residues surrounding the binuclear metal center. *Biochemistry 36*, 4934–4942.
33. Baumgrass, R., Weiwad, M., Erdmann, F., Liu, J. O., Wunderlich, D., Grabley, S., and Fischer, G. (2001) Reversible inhibition of calcineurin by the polyphenolic aldehyde gossypol. *J. Biol. Chem. 276*, 47914–47921.
34. Gille, H., Kortenjann, M., Thomae, O., Moomaw, C., Slaughter, C., Cobb, M. H., and Shaw, P. E. (1995) ERK phosphorylation potentiates Elk-1-mediated ternary complex formation and transactivation. *EMBO J. 14*, 951–962.
35. Janknecht, R., Ernst, W. H., Pingoud, V., and Nordheim, A. (1993) Activation of ternary complex factor Elk-1 by MAP kinases. *EMBO J. 12*, 5097–5104.
36. Marais, R., Wynne, J., and Treisman, R. (1993) The SRF accessory protein Elk-1 contains a growth factor-regulated transcriptional activation domain. *Cell 73*, 381–393.
37. Kayyali, U. S., Zhang, W., Yee, A. G., Seidman, J. G., and Potter, H. (1997) Cytoskeletal changes in the brains of mice lacking calcineurin A α. *J. Neurochem. 68*, 1668–1678.
38. Eastwood, S. L., Burnet, P. W., and Harrison, P. J. (2005) Decreased hippocampal expression of the susceptibility gene PPP3CC and other calcineurin subunits in schizophrenia. *Biol. Psychiatry 57*, 702–710.
39. Albert, K. A., Hemmings, H. C., Jr., Adamo, A. I., Potkin, S. G., Akbarian, S., Sandman, C. A., Cotman, C. W., Bunney, W. E., Jr., and Greengard, P. (2002) Evidence for decreased DARPP-32 in the prefrontal cortex of patients with schizophrenia. *Arch. Gen. Psychiatry 59*, 705–712.
40. Jiang, H., Xiong, F., Kong, S., Ogawa, T., Kobayashi, M., and Liu, J. O. (1997) Distinct tissue and cellular distribution of two major isoforms of calcineurin. *Mol. Immunol. 34*, 663–669.
41. Luo, C., Shaw, K. T., Raghavan, A., Aramburu, J., Garcia-Cozar, F., Perrino, B. A., Hogan, P. G., and Rao, A. (1996) Interaction of calcineurin with a domain of the transcription factor NFAT1 that controls nuclear import. *Proc. Natl. Acad. Sci. U.S.A. 93*, 8907–8912.
42. Martinez-Martinez, S., Rodriguez, A., Lopez-Maderuelo, M. D., Ortega-Perez, I., Vazquez, J., and Redondo, J. M. (2006) Blockade of NFAT activation by the second calcineurin binding site. *J. Biol. Chem. 281*, 6227–6235.
43. Li, H., Zhang, L., Rao, A., Harrison, S. C., and Hogan, P. G. (2007) Structure of calcineurin in complex with PVIVIT peptide: Portrait of a low-affinity signalling interaction. *J. Mol. Biol. 369*, 1296–1306.
44. Liu, L., Zhang, J., Yuan, J., Dang, Y., Yang, C., Chen, X., Xu, J., and Yu, L. (2005) Characterization of a human regulatory subunit of protein phosphatase 3 gene (PPP3RL) expressed specifically in testis. *Mol. Biol. Rep. 32*, 41–45.
45. Muramatsu, T., and Kincaid, R. L. (1992) Molecular cloning and chromosomal mapping of the human gene for the testis-specific catalytic subunit of calmodulin-dependent protein phosphatase (calcineurin A). *Biochem. Biophys. Res. Commun. 188*, 265–271.
46. Cottrell, J. R., Li, B., and Gerber, D. J. (2006) Calcineurin Aγ is expressed in the brain and forms a functional phosphatase. Georgia World Congress.
47. Gooch, J. L., Barnes, J. L., Garcia, S., and Abboud, H. E. (2003) Calcineurin is activated in diabetes and is required for glomerular hypertrophy and ECM accumulation. *Am. J. Physiol. 284*, 144–154.
48. Buttini, M., Limonta, S., Luyten, M., and Boddeke, H. (1995) Distribution of calcineurin A isoenzyme mRNAs in rat thymus and kidney. *Histochem. J. 27*, 291–299.
49. Kuno, T., Mukai, H., Ito, A., Chang, C. D., Kishima, K., Saito, N., and Tanaka, C. (1992) Distinct cellular expression of calcineurin Aα and Aβ in rat brain. *J. Neurochem. 58*, 1643–1651.
50. Kelly, M. A., Chellgren, B. W., Rucker, A. L., Troutman, J. M., Fried, M. G., Miller, A. F., and Creamer, T. P. (2001) Host-guest study of left-handed polyproline II helix formation. *Biochemistry 40*, 14376–14383.
51. Huai, Q., Kim, H. Y., Liu, Y., Zhao, Y., Mondragon, A., Liu, J. O., and Ke, H. (2002) Crystal structure of calcineurin-cyclophilin-cyclosporin shows common but distinct recognition of immunophilin-drug complexes. *Proc. Natl. Acad. Sci. U.S.A. 99*, 12037–12042.
52. Guerini, D., and Klee, C. B. (1989) Cloning of human calcineurin A: Evidence for two isozymes and identification of a polyproline structural domain. *Proc. Natl. Acad. Sci. U.S.A. 86*, 9183–9187.
53. Hou, Q., Yi, X., Jiang, G., and Wei, Q. (2004) The salt bridge of calcineurin is important for transferring the effect of CNB binding to CNA. *FEBS Lett. 577*, 294–298.

BI8019355